Relative angle determinable stitching interferometry for hard x-ray reflective optics

Hidekazu Mimura,[a] Hirokatsu Yumoto, and Satoshi Matsuyama
Department of Precision Science and Technology, Graduate School of Engineering, Osaka University, 2-1 Yamada-oka, Suita, Osaka 565-0871, Japan

Kazuya Yamamura
Research Center for Ultra-Precision Science and Technology, Graduate School of Engineering, Osaka University, 2-1 Yamada-oka, Suita, Osaka 565-0871, Japan

Yasuhisa Sano and Kazumasa Ueno
Department of Precision Science and Technology, Graduate School of Engineering, Osaka University, 2-1 Yamada-oka, Suita, Osaka 565-0871, Japan

Katsuyoshi Endo and Yuzo Mori
Research Center for Ultra-Precision Science and Technology, Graduate School of Engineering, Osaka University, 2-1 Yamada-oka, Suita, Osaka 565-0871, Japan

Makina Yabashi
SPring-8/Japan Synchrotron Radiation Research Institute (JASRI), 1-1-1 Kouto, Mikazuki, Hyogo 679-5148, Japan

Kenji Tamasaku, Yoshinori Nishino, and Tetsuya Ishikawa
SPring-8/RIKEN, 1-1-1 Kouto, Mikazuki, Hyogo 679-5148, Japan

Kazuto Yamauchi
Department of Precision Science and Technology, Graduate School of Engineering, Osaka University, 2-1 Yamada-oka, Suita, Osaka 565-0871, Japan

(Received 27 September 2004; accepted 17 January 2005; published online 16 March 2005)

Metrology plays an important role in surface figuring with subnanometer accuracy. We have developed relative angle determinable stitching interferometry for the surface figuring of elliptical mirrors, in order to realize hard x-ray nanofocusing. In a stitching system, stitching angles are determined not by the general method using a common area between neighboring shots, but by the new method using the mirror's tilt angles measured at times when profile data are acquired. The high measurement accuracy of approximately 4 nm (peak-to-valley) was achieved in the measurement of a cylindrical surface having the same curvature as the elliptically designed shape to enable hard x-ray nanofocusing. © *2005 American Institute of Physics.* [DOI: 10.1063/1.1868472]

I. INTRODUCTION

Recently, by utilizing hard x rays obtained by third-generation synchrotron radiation facilities, the performances of various applications have been advanced significantly. Hard x-ray imaging techniques, such as holography, phase contrast imaging and refraction contrast imaging, are powerful methods for nondestructive analysis of the inner structures of materials and are used in various fields including the medical, biological, and material sciences. In scanning hard x-ray microscopy with high lateral resolution, a focused x-ray beam is often employed. The techniques presently available for generating a small spot size are based on total reflection or diffraction. Total reflection mirrors are attractive optics because of the absence of chromatic aberration and the use of a high-brightness beam. The Kirkpatrick–Baez (K-B) mirror system consisting of two elliptical mirrors is used for two-dimensional focusing.[1–4] However, a major obstacle to the use of the K-B mirror system is the need to create elliptical surfaces having nanometer-level accuracy.

A large variety of fabrication methods for highly accurate figuring, such as ion beam figuring and differential deposition, have been developed.[3,5] We have also established a fabrication system constructed by plasma chemical vaporization machining (PCVM) and elastic emission machining (EEM).[6,7] This system can create mirror surfaces with peak-to-valley (PV) accuracies as high as 1 nm and a lateral resolution close to 0.1 mm, when the thickness to be removed is known with a required degree of accuracy.[8] Therefore, the improvement in the performance of a metrology technique plays the most important role in the advancement of figure accuracy not only at x-ray mirror surfaces but also at other optical surfaces.

Yamauchi *et al.* developed microstitching interferometry (MSI), in which microscopic and large-area phase-shifting interferometers are compositely utilized, to measure the sur-

[a]Electronic mail: mimura@prec.eng.osaka-u.ac.jp

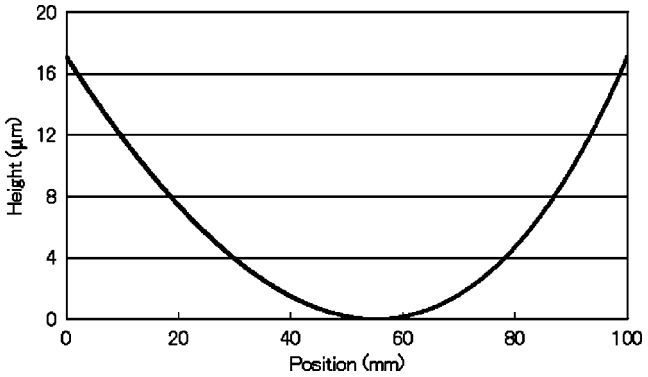

FIG. 1. Surface profile of x-ray nanofocusing mirror having large numerical aperture. The parameters of this profile are shown in Table I.

face profiles of x-ray mirrors with a PV accuracy higher than 1 nm and with a spatial resolution close to 20 μm.[9] Total-reflection mirrors have such steep rectangular shapes that the number of stitches in the longitudinal direction exceeds 30 in the case of measuring the entire area using the microscopic interferometer. The Fizeau interferometer, which can measure a large-area profile in one shot, is used to compensate for the stitching angles. Flat and elliptical mirrors have been fabricated by computer-controlled machining using PCVM and EEM on the basis of surface profiles obtained by MSI. The flat mirror has been confirmed to have an efficiently flat intensity distribution in a totally reflected beam having a wavelength of 0.06 nm at the 1-km-long beamline of SPring-8.[10] The focusing mirror having an elliptical shape has been confirmed to have a diffraction-limited focusing performance at the same beamline.[11] The full width at half maximum (FWHM) of the focal beam profile was 180 nm. In addition, the focal beam profile has been confirmed to agree well with the beam profiles predicted by calculating the Fresnel–Kirchhoff integral while taking the measured surface profile into account, not only in terms of focal size but also in terms of the shape of the intensity distribution, including the satellite peak structures. A K-B mirror system using fabricated mirrors has been constructed and confirmed to enable 200×200 nm focusing of 15 keV x rays.[4,6] These results indicate the effectiveness of the fabrication system using MSI.

To realize a smaller focal size, more steeply curved elliptical mirrors having a larger glancing angle should be designed and fabricated, taking the numerical aperture into account. As described later, we designed an elliptical nanofocusing mirror with a performance in which the FWHM of the focal profile is approximately 30 nm at diffraction limited focusing. However, in the measurement using the Fizeau interferometer, when the angle between a tested surface and a flat reference plate surface exceeds approximately 1×10^{-4} rad, the density of the interference fringes is so high that the tested surface profile cannot be measured. This denotes that the designed profile cannot be obtained by one-shot measurement with high accuracy in long spatial wavelength ranges.

In this study, we developed the relative angle determinable stitching interferometry (RADSI) using the Fizeau interferometer, for the measurement of an elliptical x-ray mirror more steeply curved than previously fabricated elliptical mirrors. In the stitching system, stitching angles are determined not by the general method using a common area between neighboring shots, but by the method using the mirror's tilt angles measured at times when profile data are acquired.

A cylindrical mirror surface having the same curvature as the designed profile was used to evaluate the performance. By comparing the two surface profiles measured by setting the mirror normally and inversely, the PV of the differential profile between the two profiles was achieved to be 4 nm.

TABLE I. Parameters of the mirror designed to enable nanofocusing.

Substrate material	CZ-(111)Si single crystal
Surface coating	Pt
Effective mirror size in longitudinal direction	100 mm
Length of ellipse	500.075 m
Breadth of ellipse	44.7 mm
Focus length	128 mm
Glancing angle on optical axis	3.65 mrad
Maximum glancing angle	4.47 mrad

II. DESIGN OF ELLIPTICAL PROFILE AND INVESTIGATION OF REQUIRED FIGURE ACCURACY FOR NANOMETER HARD X-RAY FOCUSING

We designed the shape of an elliptical mirror of 100 mm length and 150 nm focal length in order to realize a nanometer-size focused hard x-ray beam at the 1-km-long beam line (BL29XUL) of SPring-8.[12,13] The figure profile and employed ellipse parameters are shown in Fig. 1 and Table I, respectively. The incident x-ray energy and glancing angle were set at 15 keV and 3.65 mrad, respectively. Figure 2 shows the wave-optically calculated intensity profile of the beam focused by the ideally shaped ellipse for the case that the incident slit width is 100 μm and the transverse coherence length is 50 μm. The FWHM and the interval between the first two minima are found to be 28 and 50 nm, respectively. To investigate the mutual relationship between the degree of figure errors and the focusing performances, we calculated the focused beam profiles using three ellipse profiles having three figure errors as mirror surfaces. The figure errors are characterized in short, middle, and long spatial wavelength ranges relevant to 2–5, 10–20, and 20–50 mm,

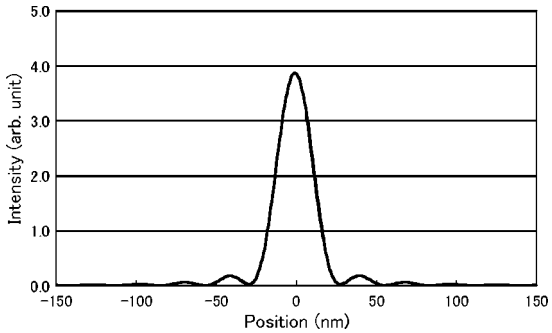

FIG. 2. Intensity profile of ideally focused x-ray beam at 15 keV. This profile is calculated by a wave optical simulator based on the Fresnel–Kirchhoff integral.

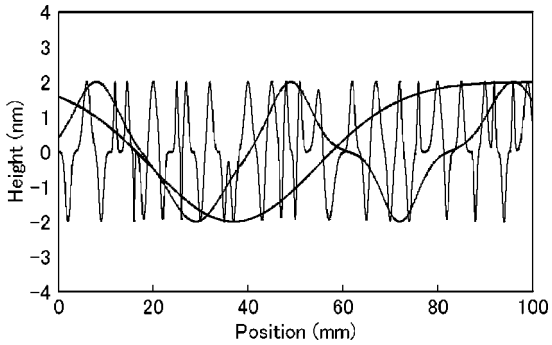

FIG. 3. Figure error profiles characterized in short, middle, and long spatial wavelength ranges to be used in the investigation of the relation between the nature of figure errors and the uniformity of focusing x-ray beams.

respectively. The PV heights of the figure errors are 4 and 6 nm in each profile. Figure 3 shows the employed figure error profiles having 4 nm (PV). Figure 4(a) shows the calculated intensity profiles on the focal plane when the height error is 4 nm. Figure 4(b) shows the intensity profiles when the height error is 6 nm. These figures indicate that to achieve the ideal FWHM, the degree of figure accuracy should be under 4 nm (PV). In particular, the figure errors in the middle spatial wavelength ranges deform the shape of the focal beam profiles.

The results of these analyses indicate that a measurement accuracy of at least 4 nm (PV) is necessary for the employed metrology.

III. HIGHLY ACCURATE STITCHING TECHNOLOGY

A. Stitching concept

There are many types of surface testing methods for aspheric optics.[14,15] In this study, as mentioned above, stitching

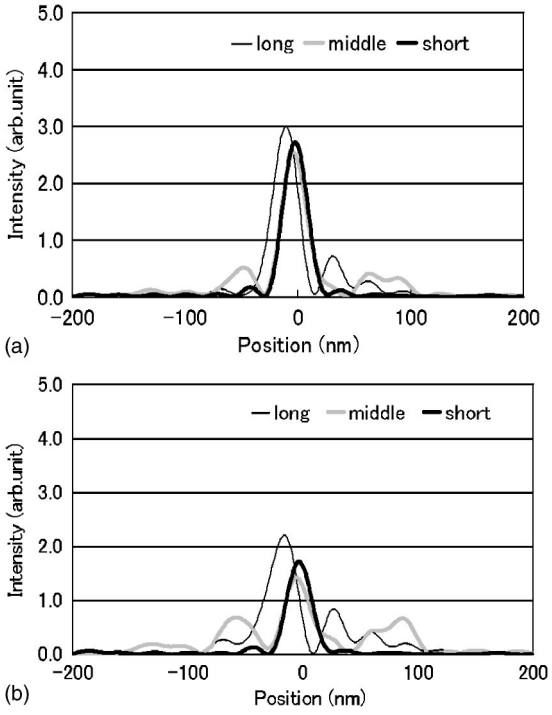

FIG. 4. Calculated intensity profiles of focused x-ray beams using the elliptical mirror having figure errors characterized in short, middle, and long spatial wavelength ranges. (a) Height error: 4 nm, (b) height error: 6 nm.

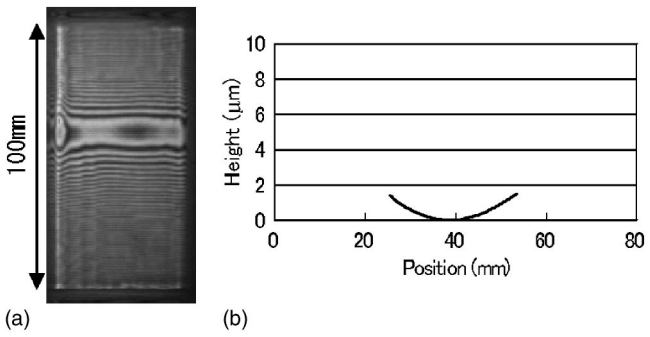

FIG. 5. Interference fringe pattern of the cylindrical mirror having the same curvature as the designed elliptical mirror as shown in Fig. 1. (a) Interference fringe pattern. (b) Measured surface profile.

technologies using an optical interferometer have been applied for the measurement of elliptical surface profiles.

Figure 5(a) shows an interference fringe pattern in the measurement of the cylindrical surface having almost the same curvature as the designed elliptical profile shown in Fig. 1. Figure 5(b) shows the surface profile measured in one shot using the Fizeau interferometer (ZYGO GPI-XP HR). On the mirror surface except for the central part, the density of the interference fringes is so high that the surface profile cannot be acquired, and that the length of the measurable area in the longitudinal direction of the mirror surface is only approximately 30 mm. In the measurement using the employed Fizeau interferometer, it is impossible to measure the surface profile if the angle between the tested surface and the reference plate surface exceeds 1×10^{-4} rad. When we attempted to measure this profile using the Fizeau interferometer, the only way to create the surface profile of the entire area is stitching as many partial surface profiles as required to cover the entire area, which are obtained by shifting the position of the measurable area.

In the conventional stitching method, each profile is stitched by minimizing the root mean square of the superposition error between neighboring shots. The following plane functions are calculated and used to minimize the superposition error:

$$f(x,y) = ax + by + c. \tag{1}$$

This function is calculated at every superposition area. When x and y are positional coordinates in the longitudinal and transverse directions on the mirror, a and b correspond to the stitching angles between the neighboring surface profiles in the longitudinal and transverse directions, respectively. On the other hand, c corresponds to the difference in the position in the vertical direction between neighboring shots. As mentioned in the previous article concerning the development of MSI,[9] the problem associated with creating the surface profile by the conventional stitching method is that the inclusion of low-frequency error is unavoidable in the finally stitched surface profile. The reason behind this problem is that each stitching angle error is integrated in continuously stitching each measured profiles. Each stitching angle error originates from a slight mismatch in the superposition area between neighboring shots.

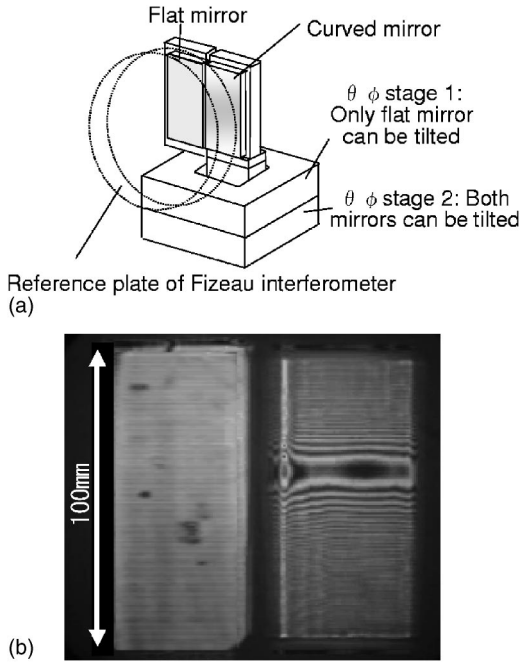

FIG. 6. Schematic drawing of mirrors inclining stages and interference fringe patterns in surface figure measurement. (a) Schematic drawing. (b) Interference fringe pattern.

In this case, since the density of the interference fringe pattern is high, as shown in Fig. 5(a), the measurement error is so large in the short spatial wavelength ranges that coefficients having a large degree of error are calculated. To evaluate the reproducibility of a, b, and c calculated using the superposition area between two neighboring profiles partially measured on a steeply curved mirror, as shown in Fig. 5, three sets of neighboring surface profiles were measured individually and three sets of each calculated coefficient were compared. Even if the length of the superposition area was two-thirds that of the measured area, the PVs of the calculated a and b were 2.1×10^{-7} and 1.9×10^{-7} rad, respectively. On the other hand, the degree of repeatability in the calculation of c was confirmed to be less than 1 nm (PV). Since unidirectional stitching is necessary to create the surface profiles of x-ray mirrors, it is necessary to improve the accuracy of the calculated a. a must have a high accuracy of 1×10^{-8} rad to achieve the above-mentioned measurement accuracy, considering that stitching errors are integrated in the creation of the entire surface profile.

B. Relative angle determinable stitching system

To measure the partial surface profile of each part on the elliptical mirror surface continuously, the mirror needs to be tilted by a constant angle in the interval between each measurement. Because coefficient a in function (1) corresponds to the angle by which the mirror is tilted, obtaining each a with an accuracy of 1×10^{-8} rad can be equated to measuring each tilt angle with an accuracy of 1×10^{-8} rad. When the figure of a tested surface is nearly flat, the angle between the tested surface and the reference plate surface can be determined directly from the measured surface profile without the process of plane correction. By comparing with the angles obtained in the consecutive measurements, the obtainable angles were confirmed to have a repeatability of 1×10^{-8} rad level.

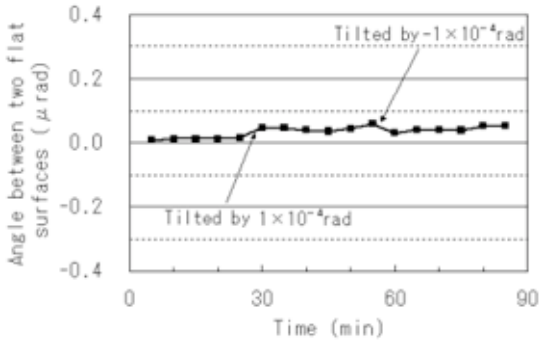

FIG. 7. Repeatability of the measured angles between flat mirror surfaces placed on two stages. Relative angles are calculated by using surface profiles without plane correction.

In this study, the system using a flat mirror to measure the differences in tilt angles between before and after the tested mirror is tilted, at the accuracy of 1×10^{-8} rad, is proposed and installed in the Fizeau interferometer. In the system, the angles are calculated on the basis of the surface profiles, without plane correction, of the flat mirror tilted together with the curved mirror. Figure 6(a) shows the schematic illustration of the newly installed stage. This stage is made up of two mirror holders and two θ ϕz piezoelectric stages (PI-Polytec. Co., P-528, TCD) used to incline the two mirrors. This construction enables the lower piezoelectric stage to incline the two mirrors together, and the upper stage to incline only the flat mirror. Figure 6(b) shows the interference fringe patterns in the measurement of surface profiles. This figure indicates that both surface profiles of the two mirrors can be acquired simultaneously. The relative angle between the two mirrors' surfaces should be kept constant during the measurement of the required number of surface profiles to cover an entire area, even if the two mirrors are tilted simultaneously by using the lower stage. To investigate the fluctuation of the relative posture between the two mirrors' surfaces on the two stages, flat mirrors were set on both tables. Figure 7 shows the relationship between the measured relative angles and time. After 30 min from the start of the measurement, both mirrors were tilted by 1×10^{-4} rad using the lower piezoelectric stage, and after 60 min, they were tilted inversely back by the same angle. The measured relative angles between the two surfaces are found to be stably kept within the 3×10^{-8} rad level over a period of approximately 90 min, despite both mirrors being tilted by 1×10^{-4} rad for 30 min during this period. As many partial surface figure profiles as required to cover the entire area of an elliptical mirror are acquired by carrying out the procedure hereinafter described. In the preparatory stage, the interference fringe pattern between two surfaces of the curved mirror and the reference plate is formed by adjusting the tilt angle of the tested mirror using the lower piezoelectric stage so that the surface profile on the edge area of the mirror surface can be measured. The tilt angle of the flat mirror surface is also adjusted using the upper piezoelectric stage so

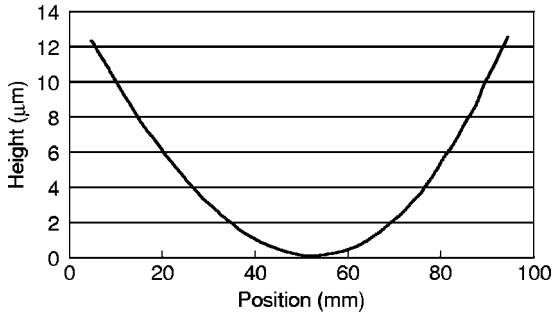

FIG. 8. Measured surface profile of cylindrical mirror having the same curvature as designed elliptical surface profile. This profile is the result of stitching many partial profiles using the relative angles determined at surface profile acquisition.

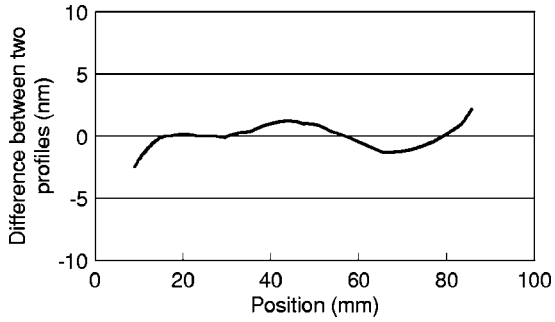

FIG. 10. Differential profile between two measured surface figure profiles of the cylindrical mirror in the normal and inverted mirror positions. High-frequency error was climinated using the surface profile obtained using MSI.

that the surface profile of the flat mirror can be measured. The measurement data, in which both the partial surface profile of the tested mirror and the entire surface profile of the flat mirror are included, is thus acquired. To render the neighboring area readily measurable, both mirrors are tilted using the lower piezoelectric stage, in which the tilt angle is determined by considering the area size of each superposition area between the neighboring profiles. The tilting of both mirrors and the measurement of surface profiles are repeated alternately until the angle between the two surfaces of the flat mirror and the reference plate becomes approximately 1×10^{-4} rad. When the angle reaches 1×10^{-4} rad, the flat mirror alone is tilted inversely by 2×10^{-4} rad, using the upper piezoelectric stage. These processes are carried out continuously. Each partial surface profile is digitally stitched using the newly coded program. In this code, only *a* in function (1) is determined using the tilt angles of the tested mirror estimated on the basis of the surface profiles of the flat mirror, and *b* and *c* are determined using each superposition area between neighboring shots.

IV. EVALUATION OF PERFORMANCES AND DISCUSSION

The cylindrical mirror shown in Fig. 5 was employed to demonstrate the RADSI. To evaluate the measurement repeatability in the obtained stitched profiles, two sets of measurements were carried out continuously at the same mirror position and the two obtained profiles were compared. The

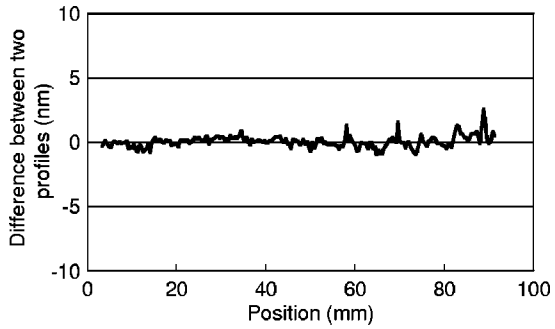

FIG. 9. Differential profile between two measured surface figure profiles of the cylindrical mirror at the same position. The two profiles are measured continuously. Degree of measurement reproducibility is less than 2 nm (PV).

developed system was placed on the vibration isolation stage in the room, where the temperature was maintained constant within ±0.5 deg centigrade. The number of stitches was approximately 30 and the length of each superposition area was set to be at least two-thirds that of each measured area. Figures 8 and 9 show the measured surface profiles of the cylindrical mirror and the differential profile between the two surface profiles, respectively. On the basis of these results, the developed system was confirmed to have a performance of 2 nm (PV) in the measurement repeatability at wavelength ranges longer than approximately 20 mm. To evaluate the measurement performance in greater detail, the two profiles measured under the normal and inverted positional conditions were compared. The reference plate surface profile determined by the three-surface method is subtracted from both profiles. Since a relatively short frequency measurement error is unavoidable in the measurement using the Fizeau interferometer, the error profiles are removed by combining the same-area profiles obtained using the MSI. The combination method is the same as that mentioned in the previous report regarding development of MSI.[9] Figure 10 shows the differential profile of the two profiles. The PV of the profile is found to be 4 nm.

These evaluation results indicate that the designed elliptical figure profile having the same curvature as that of the tested mirror can also be measured at the same accuracy as the figure accuracy required to realize nanofocusing having a performance of approximately 30 nm as the FWHM of the intensity profile.

In this study, we propose the concept of stitching technology. In stitching technologies, to determine highly accurate relative angles between neighboring shots is most important for increasing the low-frequency measurement accuracy in the stitched profiles. As reported earlier, when more steeply curved mirrors are measured, it becomes more difficult to accurately determine the relative angles by using only the superposition areas. In this case, the relative angles should be determined at times when profile data are acquired. Although the system developed in this study is specialized for unidirectional stitching measurements of hard x-ray focusing mirror surfaces, the concept of RADSI can be widely applied to the surface figure testing of various types of steeply curved and large-size mirrors.

ACKNOWLEDGMENTS

This research was supported by a Grant-in-Aid for Scientific Research (S), 15106003, 2004 and 21st Century COE Research, Center for Atomistic Fabrication Technology, 2004 from the Ministry of Education, Culture, Sports, Science and Technology of Japan.

[1] E. D. Fabrizio, F. Romanato, M. Gentill, S. Cabrini, B. Koullsh, J. Suslnl, and R. Barrett, Nature (London) **401**, 898 (1999).
[2] O. Hignette, G. Rostaing, P. Cloetens, A. Rommeveaux, W. Ludwig, and A. K. Freund, Proc. SPIE **4499**, 105 (2001).
[3] G. E. Ice, J. S. Chung, J. Z. Tischler, A. Lunt, and L. Assoufid, Rev. Sci. Instrum. **71**, 2635 (2000).
[4] K. Yamauchi, K. Yamamura, H. Mimura, Y. Sano, A. Saito, K. Endo, A. Souvorov, M. Yabashi, K. Tamasaku, T. Ishikawa, and Y. Mori, Jpn. J. Appl. Phys., Part 1 **42**, 7129 (2003).
[5] A. Schindler, G. Boehm, T. Haensel, W. Frank, A. Nickel, B. Rauschenbach, and F. Bigl, Proc. SPIE **4451**, 242 (2001).
[6] K. Yamamura, K. Yamauchi, H. Mimura, Y. Sano, A. Saito, K. Endo, A. Souvorov, M. Yabashi, K. Tamasaku, T. Ishikawa, and Y. Mor, Rev. Sci. Instrum. **74**, 4549 (2003).
[7] K. Yamauchi, H. Mimura, K. Inagaki, and Y. Mori, Rev. Sci. Instrum. **73**, 4028 (2002).
[8] H. Mimura, K. Yamauchi, K. Yamamura, A. Kubota, S. Matsuyama, Y. Sano, K. Ueno, K. Endo, Y. Nishino, K. Tamasaku, M. Yabashi, T. Ishikawa, and Y. Mori, J. Synchrotron Radiat. **11**, 343 (2004).
[9] K. Yamauchi, K. Yamamura, H. Mimura, Y. Sano, A. Saito, A. Souvorov, M. Yabashi, K. Tamasaku, T. Ishikawa, and Y. Mori, Rev. Sci. Instrum. **74**, 2894 (2003).
[10] Y. Mori, K. Yamauchi, K. Yamamura, H. Mimura, A. Saito, H. Kishimoto, Y. Sekito, M. Kanaoka, A. Souvorov, M. Yabashi, K. Tamasaku, and T. Ishikawa, Proc. SPIE **4501**, 30 (2001).
[11] K. Yamauchi, K. Yamamura, H. Mimura, Y. Sano, A. Saito, A. Souvorov, M. Yabashi, K. Tamasaku, T. Ishikawa, and Y. Mori, J. Synchrotron Radiat. **9**, 313 (2002).
[12] T. Ishikawa, K. Tamasaku, M. Yabashi, S. Goto, Y. Tanaka, H. Yamazaki, K. Takeshita, H. Kimura, H. Ohashi, T. Matsushita, and T. Ohata, Proc. SPIE **4154**, 1 (2001).
[13] K. Tamasaku, Y. Tanaka, M. Yabashi, H. Yamazaki, N. Kawamura, M. Suzuki, and T. Ishikawa, Nucl. Instrum. Methods Phys. Res. A **467–468**, 686 (2001).
[14] P. Z. Takacs, E. L. Church, C. J. Bresloff, and L. Assoufid, Appl. Opt. **38**, 5468 (1999).
[15] P. E. Murphy, T. G. Brown, and D. T. Moore, Appl. Opt. **39**, 2122 (2000).